

Temporal Correlation Meets Embedding: Towards a 2nd Generation of JDE-based Real-Time Multi-Object Tracking

Yunfei Zhang^{1†}, Jin Gao^{2,3†}, Chao Liang^{4,7†}, Zhipeng Zhang⁵, Weiming Hu^{1,2,3},
Stephen Maybank⁶, Xue Zhou^{4,7*}, Liang Li^{8*}

¹School of Information Science and Technology, ShanghaiTech University, 201210, Shanghai, China.

²State Key Laboratory of Multimodal Artificial Intelligence System, Institute of Automation, Chinese Academy of Sciences, 100190, Beijing, China.

³School of Artificial Intelligence, University of Chinese Academy of Sciences, 101408, Beijing, China.

⁴Shenzhen Institute for Advanced Study, University of Electronic Science and Technology of China, 518110, Shenzhen, China.

⁵KargoBot, China.

⁶Department of Computer Science and Information Systems, Birkbeck College, WC1E 7HX London, U.K..

⁷School of Automation Engineering, University of Electronic Science and Technology of China, 611731, Chengdu, China.

⁸Beijing Institute of Basic Medical Sciences, 100850, Beijing, China.

*Corresponding author(s). E-mail(s): zhouxue@uestc.edu.cn; liang.li.brain@aliyun.com;

Contributing authors: zhangyf32022@shanghaitech.edu.cn; jin.gao@nlpr.ia.ac.cn;

chaoliang1996@gmail.com; zhipeng.zhang.cv@outlook.com; wmhu@nlpr.ia.ac.cn;

sjmaybank@dcs.bbk.ac.uk;

†These authors contributed equally to this work.

Abstract

Joint Detection and Embedding (JDE) trackers have demonstrated excellent performance in Multi-Object Tracking (MOT) tasks by incorporating the extraction of appearance features as auxiliary tasks through embedding Re-Identification task (ReID) into the detector, achieving a balance between inference speed and tracking performance. However, solving the competition between the detector and the feature extractor has always been a challenge. Meanwhile, the issue of directly embedding the ReID task into MOT has remained unresolved. The lack of high discriminability in appearance features results in their limited utility. In this paper, a new learning approach using cross-correlation to capture temporal information of objects is proposed. The feature extraction network is no longer trained solely on appearance features from each frame but learns richer motion features by utilizing feature heatmaps from consecutive frames, which addresses the challenge of inter-class feature similarity. Furthermore, our learning approach is applied to a more lightweight feature extraction

network, and treat the feature matching scores as strong cues rather than auxiliary cues, with an appropriate weight calculation to reflect the compatibility between our obtained features and the MOT task. Our tracker, named TCBTrack, achieves state-of-the-art performance on multiple public benchmarks, i.e., MOT17, MOT20, and DanceTrack datasets. Specifically, on the DanceTrack test set, we achieve 56.8 HOTA, 58.1 IDF1 and 92.5 MOTA, making it the best online tracker capable of achieving real-time performance. Comparative evaluations with other trackers prove that our tracker achieves the best balance between speed, robustness and accuracy. Code is available at <https://github.com/yfzhang1214/TCBTrack>.

Keywords: Multiple object tracking, cross-correlation, lightweight networks, re-identification

1 Introduction

Multi-Object Tracking (MOT) is a crucial task in computer vision, aiming to track multiple objects robustly and accurately over time. So far, MOT has been applied in various fields, including autonomous driving(Petrovskaya and Thrun, 2009; Geiger et al, 2013; He et al, 2016; Yu et al, 2020; Luo et al, 2021; Kim et al, 2022), video surveillance (Milan et al, 2016; Dendorfer et al, 2020), and in high level tasks such as pose estimation and the prediction of human behaviour(Wu et al, 2019; Gu et al, 2019).

Tracking-by-Detection is one of the main approaches for addressing MOT tasks. It is a two-step process, with the detection of objects followed by the matching of objects(Kalman et al, 1960; Kuhn, 1955) between frames for object association. Within this paradigm, Joint Detection and Embedding (JDE) integrates the re-identification (ReID) task into the detector by adding a head branch to avoid re-extracting features from the ReID network. This integration has achieved a good balance between accuracy and speed (Wang et al, 2020; Lu et al, 2020; Pang et al, 2021; Zhang et al, 2021; Liang et al, 2022b). However, JDE trackers have an unresolved and significant shortage: directly using the same backbone as the detector results in small inter-class gaps in appearance features, which can lead to the lack of discrimination when similar objects appear in consecutive frames.

After revisiting the design process of all JDE trackers, we observe that one of the main reasons for small inter-class gaps in appearance features is that the high-dimensional features generated by the detector may not be suitable for feature extraction from specific objects. The detection

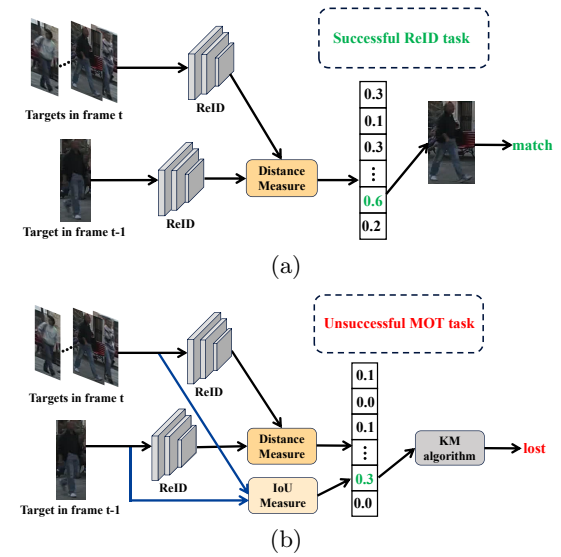


Fig. 1 Comparisons between ReID task in MOT and MOT task. (a) ReID task in MOT. (b) MOT task. The ReID task can still be accomplished effectively when embedded into the MOT algorithm, while during the association stage, matching is not performed due to the small weights. This is caused by the training approach of the ReID model, leading to the loss of temporal information, and the misalignment of weights due to the blurry templates in MOT.

backbone focuses more on the position information and classification of objects, while the feature extractor focuses more on the detailed features of objects. Previous works(Zhang et al, 2021; Liang et al, 2022b) balance these two tasks by designing richer feature extraction networks, which sacrifice speed in exchange for larger inter-class feature differences. Additionally, we have discovered similarities and differences between ReID and MOT. ReID and MOT uniquely identify individual objects. ReID finds all the images containing a given object. MOT associates target bounding boxes in the current frame with those from the



Fig. 2 Illustration of hard samples of JDE trackers. The dots in the dashed box represent the center of the object.

previous frame. However, directly embedding the ReID task into the MOT task poses certain challenges, as illustrated in Fig. 1. From the figure, the ReID model may be successful within the MOT because it finds the bounding box most similar to the target. Nevertheless, when the MOT task employs linear assignments for matching, similar candidate boxes may not be matched due to their low scores in distance measure. This phenomenon is most prevalent when the template itself is blurry or when the retrieved bounding boxes are not accurate. Many works(Wang et al, 2020; Zhang et al, 2021; Liang et al, 2022b; Cui et al, 2023) try to alleviate this issue by using linear weighting methods to obtain distance metrics and setting the weight of appearance features to a smaller value in order to assist in association. This approach leads to marginal performance improvements in tracking because the IoU metric is still an influential factor.

We aim to develop a superior method for expressing appearance features. As shown in Fig. 2, when the appearance of objects is similar, it is difficult to compensate for the mismatch caused by the inaccurate IoU metric through the distance measure of appearance features. In fact, however, the object represented by the green dot in frames can be easily tracked, as the object has been moving to the right consistently. Many Single-Object Tracking (SOT) trackers(Varior et al, 2016; Li et al, 2018, 2019) use template matching to establish motion feature responses between the template and the search region through cross-correlation operations, achieving localization of the tracked object. Inspired by siamese network in SOT, we incorporate cross-correlation into JDE structure, shown in Fig. 3. Specifically, we construct frame training pairs through video training sets and use cross-correlation operations to obtain motion heatmap for each target. Gaussian function is used to generate corresponding

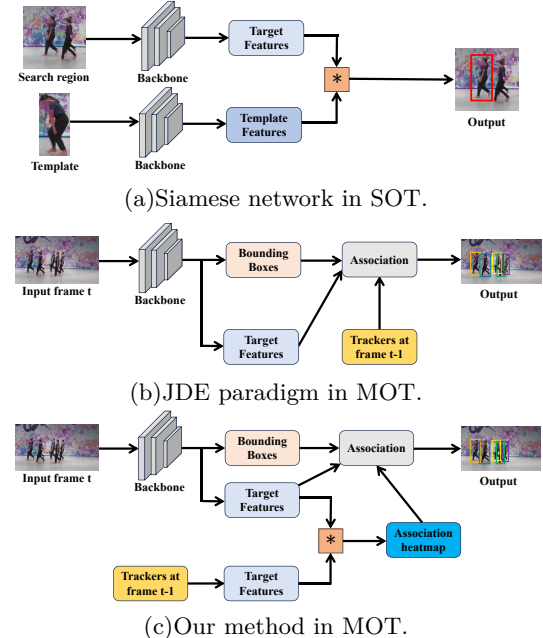


Fig. 3 The main framework of our MOT tracker. It involves incorporating object feature extraction inspired by SOT task into JDE structure, aiming to compensate for the limitations of feature extraction.

groundtruth and apply Logistic-MSE loss. The learned temporal cues alleviate the problem of feature similarity between the object and its adjacent objects. At the same time, due to the motion information, the heatmap obtained by cross-correlation has a stronger expression in continuous frames. We treat the obtained heatmap as strong motion cues, and modify the distance measure in the association stage by replacing linear weighting with product, achieving better results. We have also significantly reduced the size of the feature extraction network to gain a speed advantage.

Finally, we have designed a more lightweight JDE-based tracker, named TCBTrack (Temporal Correlation-Based Tracker). By utilizing cross-correlation, we establish temporal relationships between the consecutive frames to enrich the appearance features. Furthermore, during the association stage, similarity scores and IoU scores are measured equally. As a result, we achieve improved tracking performance. Experiments are conducted on MOT17, MOT20, and DanceTrack datasets(Milan et al, 2016; Dendorfer et al, 2020; Sun et al, 2022), and achieve state-of-the-art results. Compared to other trackers, our tracker

still exhibits the best balance in terms of robustness, accuracy, and speed.

This paper is an extension of our conference version published in AAAI'22([Liang et al, 2022a](#)). Our Previous work, OMC tracker, introduces a temporal cue training module and a re-check module. OMC applies them to recall low-confidence detection boxes to compensate for the shortcomings in detection performance. We believe that there are opportunities for research in this area. We make the following improvements to [Liang et al \(2022a\)](#):

- The object detector and the appearance model are improved. With the advancement of detectors, occluded and blurred objects can be detected more reliably, which undoubtedly provides the greatest assistance to Tracking-by-Detection paradigm trackers. Richer image features also have a promoting effect on the appearance model, so we further lightweight the appearance model.
- Temporal information from OMC is included. We have removed the re-check module used for recalling detection boxes in OMC, as the original issue has already been addressed by existing good detectors.
- A better training method for extracting the temporal features of objects is implemented, alleviating the feature similarity issue among similar objects and addressing the convergence difficulties of the ReID task in large training datasets. This approach is then applied to the appearance model.
- The association of object features over time is improved. An improved calculation method for matching scores is set up.
- The new tracker is tested on the difficult DanceTrack dataset([Sun et al, 2022](#)) and more ablation studies are added.
- More comparisons with existing trackers are described.

2 Related Work

2.1 Tracking-by-Detection Paradigm

Over the years, Tracking-by-Detection paradigm has been the focal point of MOT tasks. After object detection it is necessary to associate objects

in different frames. Early MOT methods relied on the best available detectors at the time to enhance association accuracy. IOU tracker([Bochinski et al, 2017](#)) achieves fast multi-object tracking by matching objects in adjacent frames based on Intersection over Union (IoU)([Yu et al, 2016b](#)) as the matching criterion. SORT([Bewley et al, 2016](#)), which is an improvement on the IoU tracker, introduces Kalman filter([Kalman et al, 1960](#)) and Hungarian matching algorithm([Kuhn, 1955](#)) to enhance the accuracy of the IoU-based association algorithm by predicting the objects in the next frame and reducing ID switches. DeepSORT([Wojke et al, 2017](#)) further enhances SORT by adding a feature extraction module, which extracts ReID features for each object by feeding the detected bounding boxes into a deep neural network. It then excludes associations of objects with significant distances between features, as measured by the Mahalanobis distance([Mahalanobis, 2018](#)). It is noted that early tracking tasks assume simple datasets, where the combination of Kalman Filter and IoU metric is sufficient to solve most association matching problems. Therefore, many works use ReID features as a weak cues to help eliminate matches with similar positions and sizes of bounding boxes but distinct appearance features. See [Yu et al \(2016a\)](#), [Wojke et al \(2017\)](#), [Tang et al \(2017\)](#), [Chen et al \(2018\)](#), [Aharon et al \(2022\)](#), [Wang \(2022\)](#), [Du et al \(2023\)](#), [Cui et al \(2023\)](#), [Yang et al \(2023\)](#). With the improvement of ReID techniques, differences in appearance features among different objects have become more prominent. Many trackers have utilized appearance information to obtain higher-level information and enhance object association. See [Zhang et al \(2019\)](#), [Zhou et al \(2020\)](#), [Wang et al \(2021a\)](#), [Dai et al \(2021\)](#), [Chu et al \(2023\)](#). However, as trackers strive for higher accuracy, they introduce significant additional computational overheads, making it challenging to balance precision and speed. JDE([Wang et al, 2020](#)) proposes the integration of feature extraction as a detection branch, reducing computational requirements by sharing the backbone with detectors and achieving good results in terms of performance and speed. FairMOT([Zhang et al, 2021](#)) finds JDE-based trackers which utilize a detection-learned backbone, thereby addressing the fairness issue in feature extraction and establishing a new

feature extraction network to balance the detection and feature extraction tasks. Many other trackers have similar strategies. See [Bergmann et al \(2019\)](#), [Lu et al \(2020\)](#), [Pang et al \(2021\)](#), [Liang et al \(2022b\)](#). From these developments, it is evident that extracting features efficiently and accurately has become the crucial objective of Tracking-by-Detection.

2.2 MOT Methods With Feature Extraction

For methods that rely solely on bounding boxes for motion prediction([Bewley et al, 2016](#); [Zhang et al, 2022](#); [Yi et al, 2023](#); [Cao et al, 2023](#); [Yang et al, 2023](#); [Liu et al, 2023b](#)), the quality of the detection boxes is crucial. However, there may be errors in the detection boxes if there are high speed object motions or large occlusions. To address this degradation, some approaches incorporate temporal cues from previous and future frames. For instance, [Brasó and Leal-Taixé \(2020\)](#), [Cetintas et al \(2023\)](#) leverage graph neural networks to establish object connections between frames. However, these methods require the entire video sequence as input to capture global temporal associations, which makes them unsuitable for online tracking.

Other methods([Zhang et al, 2021](#); [Pang et al, 2021](#); [Yang et al, 2021](#); [Liang et al, 2022b](#); [Aharon et al, 2022](#); [Du et al, 2023](#); [Maggiolino et al, 2023](#)) enhance deep learning networks to obtain appearance features by employing improved feature extraction networks to increase inter-class differences. Most JDE Trackers use a multi-layer perceptron (MLP) to map to the ID dimensions during training and employ ID loss for learning ([Wang et al, 2020](#); [Zhang et al, 2021](#); [Liang et al, 2022b](#); [Yu et al, 2022](#)). As a consequence, as the training sample size increases, the structure of the MLP also changes due to the increase of objects, making it difficult for the feature extractor to converge when dealing with the large training sets. Additionally, the feature extraction network remains limited to single frames in which ReID only learns appearance. As a result, features generated through the feature extraction network are not effective in discerning multiple overlapped or closely positioned objects and only play an auxiliary role during the association stage. Some

methods([Aharon et al, 2022](#); [Du et al, 2023](#); [Maggiolino et al, 2023](#)) also use triplet loss([Schroff et al, 2015](#)) to train the ReID model. Nevertheless, selecting effective triplets can be challenging for JDE trackers in MOT datasets, particularly in the presence of occlusions, motion crossovers, and scene variations: the low sensitivity of triplet loss to hard samples may lead to instability and degraded performance of the feature extractor(See [Wang et al \(2020\)](#)).

Additionally, there are works that integrate SOT methods into the MOT task. This is because SOT trackers exhibits higher requirements for feature details during matching and faces common challenges in tracking tasks, such as occlusions and irregular motion. Among them, trackers that use siamese network utilize feature matching to locate the object position, which it is not limited by the detection. Early trackers([Chu et al, 2017](#); [Sadeghian et al, 2017](#); [Zhu et al, 2018](#); [Zheng et al, 2021](#)) draw inspiration from SiamFC([Bertinetto et al, 2016](#)) and employ siamese networks to generate temporal information, replacing the traditional appearance modeling algorithms for MOT associations. Unfortunately, these trackers have a high computational complexity, because each located object has to be compared with all the tracked objects. This limitation makes them unsuitable for real-time applications. Also inspired by SOT, our previous work OMC([Liang et al, 2022a](#)) is the first to use a siamese network and similarity matching to obtain reliable information from poorly detected bounding boxes. OMC incorporates object detection, temporal feature extraction, and object recall into a unified network, making it suitable for online real-time applications and transferrable to other trackers of the same Tracking-by-Detection paradigm to improve performance. With recent advancements in object detection models([Girshick, 2015](#); [Ren et al, 2015](#); [He et al, 2017](#); [Lin et al, 2017a,b](#); [Redmon and Farhadi, 2018](#); [Ge et al, 2021](#)), the performance boost obtained by including poorly detected bounding boxes is reduced. To explore other expressions of the siamese network, we introduce a refined version of OMC, named TCBTrack, which replaces the object detection backbone with a new, more efficient one and uses similarity matching for training and association. Unlike

other traditional ReID learning methods, similarity matching not only learns appearance information but also temporal information to make the features more discriminative. By emphasizing appearance score in the association algorithm, the performance of the tracker is further enhanced. In summary, our approach utilizes siamese network architectures to extract temporal features, enabling deployment with both subpar and strong detectors while maintaining robustness and high-speed capability.

2.3 Other MOT Methods

Vision transformer (ViT)([Dosovitskiy et al, 2020](#)) is an example of a transformer that has been applied to many computer vision tasks([Carion et al, 2020](#); [Hatamizadeh et al, 2022](#); [Zhai et al, 2022](#)). It introduces the concept of treating image patches as tokens and extracting image features using transformers, demonstrating the capability of transformers in the domain of image extraction. The Detection Transformer (DETR)([Carion et al, 2020](#)) further expands the applicability of transformers in computer vision. It considers the input to the encoder part of the transformer as object queries, which are obtained by summing learnable positional encodings with image features extracted through a CNN network. The decoder part, along with prediction heads, then generates bounding boxes and confidence scores for each query, enabling end-to-end object detection. Subsequently, the Multiple Object Tracking Transformer (MOTR)([Zeng et al, 2022](#)) introduces modifications to the DETR model which are specifically tailored for MOT tasks. Traditional detection-based tracking algorithms often separate the detection and association tasks. The associations of the objects often rely on traditional mathematical methods that lack generality. MOTR proposes leveraging a similar model structure to DETR to incorporate temporal modeling capabilities for MOT tasks.

MOTR is a popular framework for end-to-end object tracking. MOTRv2([Zhang et al, 2023](#)), for example, extends MOTR by combining it with YOLOX([Ge et al, 2021](#)), resulting in an improvement in tracking performance. Besides, there are other similar methods such as [Li et al \(2023\)](#), [Yu et al \(2023\)](#), [Gao and Wang \(2023\)](#) which have also

Table 1 MOT method comparison.

Algorithms	speed	online	robust
Transformer-based	✗	✓	✓
TBD-based ¹ (motion)	✓	✓	✗
TBD-based ¹ (SDE ²)	✗	✓	✓
TBD-based ¹ (JDE)	✓	✓	✓
GNN-based	✓	✗	✓

¹TBD: Abbreviation of “Tracking-by-Detection”

²SDE: Abbreviation of “Separate Detection and Embedding”

demonstrated the success of the DETR paradigm in object tracking tasks.

Based on the ViT architecture, tracking frameworks show promising performance. Nevertheless, there are still difficulties, for example the stacking of the transformer networks and the requirement of long sequences of features as token inputs. End-to-End models consistently suffer from a speed disadvantage([Liu et al, 2023a](#); [Liu and Abbeel, 2024](#)). This is because the object association between frames and object detection are learned within the same network, necessitating more complex and larger models in support. To address this issue, some works propose using Graph Neural Networks (GNNs) for inter-frame object association, such as [Brasó and Leal-Taixé \(2020\)](#), [Liu et al \(2020\)](#), [Li et al \(2020\)](#), [Papakis et al \(2020\)](#), [Cetintas et al \(2023\)](#). These approaches employ GNNs to compute object box information (e.g., aspect ratio, size, position, confidence) and derive inter-frame weights or establish trackers between consecutive frames, enabling concatenation through the GNN framework. Unfortunately, these GNN-based methods require the entire video sequence as input, rendering them incapable of achieving online tracking. Currently, researchers are actively exploring more efficient approaches to tackle online object tracking. All types of trackers have been classified as shown in Table 1.

3 Methodology

Tracking-by-Detection. In the inference stage, one single video frame I^t is fed into the neural network. Similar to conventional Tracking-by-Detection methods, a high-dimensional feature map f^t is extracted from I^t using the detection backbone Φ . Subsequently, object detection and prediction of bounding boxes and confidence

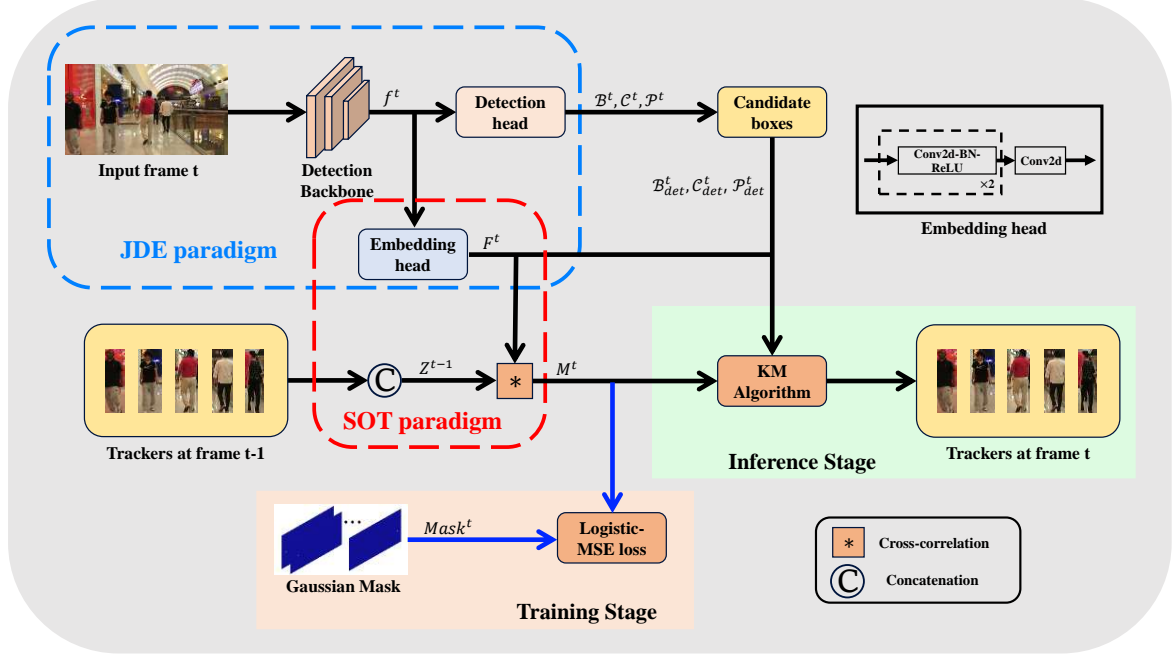


Fig. 4 Overview of the proposed TCBTrack. It consists of the JDE paradigm, the SOT paradigm and our training/inference stage (the blue arrows represent the process during the training stage.). The Detection Backbone first generates the detection result $\mathcal{B}^t, \mathcal{C}^t, \mathcal{P}^t$ and candidate embeddings F_t^{id} . We use a Gaussian heatmap and Logistic-MSE loss in the training stage, and the joint scores of heatmap, IoU, and confidence are used as weights in the inference stage.

scores are achieved by the detection head Ψ represented as:

$$f^t = \Phi(I^t), \quad (1)$$

$$[\mathcal{B}^t, \mathcal{C}^t, \mathcal{P}^t] = \Psi(f^t). \quad (2)$$

$\mathcal{B}^t \in \mathbb{R}^{H \times W \times 4}$ is the predicted position of the objects after the image frame passes through the backbone and head, $\mathcal{C}^t \in \mathbb{R}^{H \times W \times \text{class}}$ is the class probability prediction for each bounding box, and $\mathcal{P}^t \in \mathbb{R}^{H \times W \times 1}$ is the confidence prediction for each bounding box. To efficiently obtain feature vectors for each independent candidate box, we adopt the feature extraction method from JDE, which involves sharing the backbone required for feature extraction with the detector, and incorporating an additional head branch Ω for feature extraction as follows:

$$F^t = \Omega(f^t), \quad (3)$$

where $F^t \in \mathbb{R}^{H \times W \times C_{out}}$ represents the feature vectors corresponding to all candidate boxes, with each bounding box $F_i^t \in \mathbb{R}^{1 \times 1 \times C_{out}}$ possessing a feature of dimension C_{out} .

After obtaining the candidate box positions, confidence scores, classification predictions, and

feature vectors for I^t , all candidate boxes are subjected to non-maximum suppression (NMS) to filter out the final candidate boxes based on a combination of confidence and classification probability, expressed as:

$$\mathcal{S}_i^t = \mathcal{P}_i^t \cdot \max(\mathcal{C}_i^t(0), \mathcal{C}_i^t(1), \dots, \mathcal{C}_i^t(\text{class} - 1))_{i=1}^n, \quad (4)$$

$$[\mathcal{B}_{det}^t, \mathcal{C}_{det}^t, \mathcal{P}_{det}^t] = NMS([\mathcal{B}^t, \mathcal{C}^t, \mathcal{P}^t], \mathcal{S}^t) \quad (5)$$

\mathcal{S}_i^t is the overall score of each bounding box. The filtered candidate boxes are used in the tracking association stage. We have defined an embedded feature extraction method that performs well for any detector; this ensures that we can easily achieve a lightweight tracker to meet real-time requirements while ensuring accuracy. Furthermore, we simplify the embedding head with our new learning method, enabling the model to utilize better detectors under speed requirements.

3.1 TCBTrack architecture

The accuracy of the detector is a significant factor in Track-by-Detection. When the accuracy of the

detector is low, the bottleneck in MOT is the setting of a threshold for detecting bounding boxes. When the accuracy of the detector is high, the bottleneck in MOT is the description of the complex motions of objects. It is traditional to use the Kalman filter to predict the positions of objects in the next frame(Bewley et al, 2016; Yu et al, 2016a; Bochinski et al, 2017, 2018; Wang et al, 2020; Zhang et al, 2022). However, Kalman filtering is not robust in complex environments. Our inspiration comes from the experimental results of the low-detection model(Liang et al, 2022a): the heatmap obtained through cross-correlation learning can be used to find objects missed by the detector. Embedding the appearance model into MOT does not provide significant improvements, hence most methods still use IoU as the core because it is considered as strong cues for matching. Cross-correlation, aiming to utilize the motion information and appearance information of the object for feature matching, can also provide strong cues for association. Therefore, we also have enhanced the proportion of our generated features obtained in the association stage to achieve better tracking performance. The entire training stage and inference stage of TCBTrack can be seen in Fig. 4.

Embedding head. In JDE, the embedding head transforms the high-dimensional features used for detection into unique feature vectors for the objects. Just as the detector outputs the confidence, classification, and detection box position of the objects through multiple head branches, the feature vectors of the candidate boxes can also be obtained after the detection backbone. Considering the importance of the detector for MOT, we choose to simplify the computational overhead of the embedding head as much as possible and obtain better performance through specific training methods. Here, we choose to set the embedding head composed of two Conv2d-BN-ReLU layers with 3×3 convolutional kernels, and use one 1×1 convolutional kernel Conv2d to map the dimensions to the dimension of the feature vector(we take dim=512).

Transductive Detection Module. The transductive detection module aggregates the object features from the previous frame and the candidate box features from the current frame to obtain a temporal cue map. As in SiamFC there are k

templates, denoted as $z_1^{t-1}, z_2^{t-1}, \dots, z_k^{t-1}$. After operating equation (3), we obtain the feature vectors F^t for all candidate boxes in the current frame. Therefore, we use the operator * for box localization:

$$m_i^t = z_i^{t-1} * F^t |_{i=1}^n. \quad (6)$$

$m_i^t \in \mathbb{R}^{H \times W}$ represents the heatmap of the i -th tracker at frame t . Through k operations and concatenation, we can obtain the object localization information $\mathcal{M}^t = \{m_1^t, m_2^t, \dots, m_k^t\}$ for all templates in the current frame. It is worth noting that, since the dimension of the template is $\mathbb{R}^{1 \times 1 \times C_{out}}$, the cross-correlation operation can be modified to a simple matrix multiplication. Therefore, we can concatenate the features of all trackers to save time and obtain the heatmap for each template. The implementation details of the cross-correlation operation can be found in Algorithm 1.

Algorithm 1 Pseudocode of cross-correlation, Pytorch.

```

1: def generate_heatmap( $Z^{t-1}, F^t$ ) :
2:    $Z = Z^{t-1}.\text{view}(k, \text{cout})$ 
3:    $Z\_norm = \text{torch.linalg.norm}(Z, \text{dim}=1, \text{keepdim=True})$ 
4:    $F = F^t.\text{view}(H*W, \text{cout})$ 
5:    $F\_norm = \text{torch.linalg.norm}(F, \text{dim}=1, \text{keepdim=True})$ 
6:    $M = \text{torch.matmul}(Z, F.\text{T})$ 
7:    $M = \text{torch.div}(M, \text{torch.matmul}(Z\_norm, F\_norm.\text{T}))$ 
8:   return  $M.\text{view}(\text{cout}, H, W)$ 

```

Training. We do not make any changes in the detection model so the backbone and head of the detector are frozen throughout the training process. To train our embedding head, the following steps are followed:

1)Image pair selection. We randomly select image pairs such that the two images in each frame are separated by no more than five frames, which generates more image pairs for model training and ensures that the majority of the objects in the two images can be matched. Additionally, choosing images frames at slightly larger intervals(e.g., interval with 5 frames) allows the model

to learn richer temporal information, as the intervals reduce reliance on appearance information. This helps the model to generate high response heatmaps even when the object is moving rapidly or undergoing deformation.

2) Object selection. Firstly we perform a forward process on the $t-1$ frame's image I^{t-1} to obtain all candidate boxes \mathcal{B}^{t-1} , \mathcal{C}^{t-1} , \mathcal{P}^{t-1} , and their corresponding feature vectors F^{t-1} from the previous frame (equation (2), equation (3)). Subsequently, we use IoU in combination with ground truth \mathcal{B}_{gt}^{t-1} and \mathcal{ID}_{gt}^{t-1} for candidate box selection, thereby obtaining object box features and IDs of the previous frame, as detailed in Algorithm 2).

Algorithm 2 Pseudocode of object selection.

Input: All bounding boxes of the previous frame \mathcal{B}^{t-1} , ground truth bounding boxes \mathcal{B}_{gt}^{t-1} , features of the bounding boxes F^{t-1} , ground truth IDs \mathcal{ID}^{t-1} , threshold α .

Output: Features of the selected objects F_{sel}^{t-1} , IDs of the selected objects \mathcal{ID}_{sel}^{t-1} .

```

1:  $index_1 = \text{argmax}(\text{IoU}(\mathcal{B}^{t-1}, \mathcal{B}_{gt}^{t-1}(i)))|_{i=1}^n$ 
2:  $scores = \max(\text{IoU}(\mathcal{B}^{t-1}, \mathcal{B}_{gt}^{t-1}(i)))|_{i=1}^n$ 
3:  $index_2 = scores > \alpha$ 
4:  $\mathcal{ID}_{sel}^{t-1} \leftarrow index_2$ 
5:  $F_{sel}^{t-1} \leftarrow [index_1, index_2]$ 
6: return  $[F_{sel}^{t-1}, \mathcal{ID}_{sel}^{t-1}]$ 

```

The process first utilizes each $b_{gt}^{t-1} \in \mathcal{B}_{gt}^{t-1}$ to generate IoU response on \mathcal{B}^{t-1} , then selects the candidate box with the highest response value and its high-dimensional feature, labeling it with the ID number. If the IoU response is less than α (set to 0.8), it signifies that the detector itself cannot produce correct candidate boxes, and such objects will not be considered. When the score is greater than α , it indicates that the detector has a bounding box capable of capturing the object (regardless of its classification probability and confidence), and therefore can be used for training. By performing the similar operation, we obtain all candidate boxes \mathcal{ID}_{sel}^t for the next frame I^t along with their corresponding \mathcal{B}^t , \mathcal{B}_{gt}^t , \mathcal{ID}_{gt}^t . Candidate boxes with the same ID across two frames are considered as training pairs:

$$Index = \{i | \mathcal{ID}_{sel}^{t-1}(i) \in \mathcal{ID}_{sel}^t\}, \quad (7)$$

$$[\tilde{F}_{sel}^{t-1}, \tilde{\mathcal{ID}}_{sel}^{t-1}] \leftarrow [F_{sel}^{t-1}, \mathcal{ID}_{sel}^{t-1}, Index]. \quad (8)$$

Additionally, through the information of IDs $\tilde{\mathcal{ID}}_{sel}^{t-1}$, the groundtruth will be updated to $\tilde{\mathcal{B}}_{gt}^t$, \tilde{F}_{gt}^t , $\tilde{\mathcal{ID}}_{gt}^t$ applicable to the training process.

3) Model forward and groundtruth generation. We perform cross-correlation computation between the obtained F^t and \tilde{F}_{sel}^{t-1} calculated from the current frame to obtain the heatmap for each object using equation (6). We use Gaussian distributions to generate the label for each groundtruth, and by concatenation, we obtain the groundtruth heatmap H^t . A single groundtruth heatmap can be expressed by the following formula:

$$h_i^t \in \mathbb{R}^{H \times W} = \exp\left(-\frac{(x-cx_i)^2 + (y-cy_i)^2}{2\sigma^2}\right) \quad (9)$$

where the location (cx_i, cy_i) can be obtained from $\tilde{\mathcal{B}}_{gt}^t(i)$, and σ is the object size-adaptive standard deviation. We do not assign the central point as 1 and assign the region outside the central point as 0. This is because adjacent candidate boxes that represent the same object contain slightly similar temporal information and cannot be rudely considered as negative samples.

4) Loss design. The calculation is similar to the siamese method for calculating the loss on the heatmap. By using cross-entropy loss between the heatmaps generated by the model and the groundtruth heatmap generated through Gaussian distribution, we can suppress the localization of objects in other positions, thereby learning temporal cues. We use Logistic-MSE Loss as our loss function, and the specific formula is as follows:

$$\mathcal{L}_{temp} = -\frac{1}{n} \sum_{(m,h)} \sum_{x,y} \begin{cases} (1 - m_{x,y}) \log(m_{x,y}), & \text{if } h_{x,y}^t \geq 1 \\ (1 - h_{x,y}^t) m_{x,y} \log(1 - m_{x,y}), & \text{else.} \end{cases} \quad (10)$$

$m_{x,y}$ represents every single point of every heatmap. We do not add any other losses to demonstrate the benefits of our training method, so the final loss can be simply represented as \mathcal{L}_{temp} . Visualization results are shown in Fig. 5. Although the surrounding candidate boxes have been suppressed, there are still other high response values. Therefore, we use IoU to measure the positional relationship between objects in the association stage to avoid incorrect matching.

Association. Since TCBTrack no longer recalls low-confidence candidate boxes through a model,

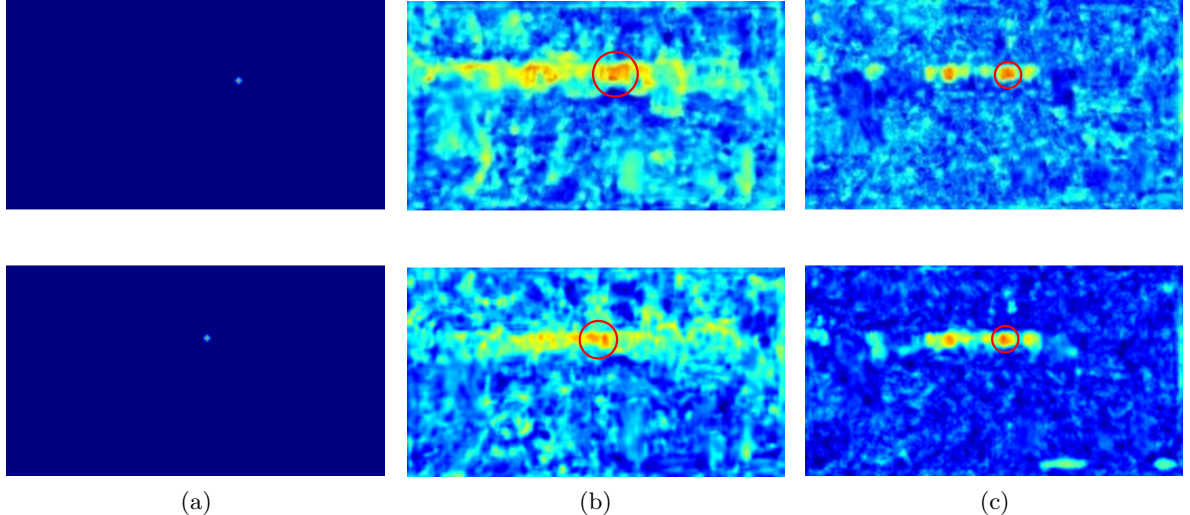


Fig. 5 Sample heatmap results using ID loss and our Logistic-MSE loss. (a) Groundtruth heatmap. (b) Heatmap generated by ID loss. (c) Heatmap generated by Logistic-MSE loss. The area circled in red represents the highest response of the heatmap. Our method can suppress the surrounding response of the target box and alleviate the problem of incorrect matching between adjacent objects.

we adopt the BYTE method of ByteTrack(Zhang et al, 2022): instead of using a threshold to filter candidate boxes, we differentiate high-confidence and low-confidence candidate boxes using the threshold. Based on the observation that occlusion is often caused by two objects with different motion characteristics, we incorporate appearance score into the calculation of association weights. We define the weights as follows:

$$Score = IoU * Det_score * Temp_score, \quad (11)$$

$$Temp_score = Cosine(F_1, F_2). \quad (12)$$

IoU is used to measure the motion characteristics between bounding boxes, while *Det_score* can treat boxes with low detection scores as unreliable objects during IoU matching to reduce the matching score. *Temp_score* is used to measure the appearance and temporal feature similarities between bounding boxes. We aim to set the matching weights in a way that allows for complementarity between motion characteristics, appearance features, and temporal features: When the IoU score is high, the challenge in MOT tasks lies in distinguishing the true object from surrounding objects, which can be addressed by appearance score. When the IoU score is low, we can also utilize it for recall. Moreover, when similar objects are connected, the temporal information

in appearance feature can be used for differentiation. This strategy is based on the premise that the object features we extracted perform well in MOT tasks and the heatmap response is high. In section 4 we compare our strategy with linear weighting scores:

$$Score = (1 - \delta) * IoU + \delta * Temp_score \quad (13)$$

Additionally, we use linear weighting method to update the features of the tracked object:

$$F^t = (1 - \gamma) * F^{t-1} + \gamma * F^t. \quad (14)$$

Here we set γ to 0.1 because experiments show that small values of γ reduce the incorrect matching of adjacent. However, if γ is too small, then the features of objects in the current frame cannot be updated. Also based on our training method, we use the cosine distance as the weight for the first stage matching. The entire tracking process is described in Algorithm 3: Three associations are used to match the current frame with the tracked object from the previous frame. *Association1* uses equation (11) to match most of the objects, and then *Association2* and *Association3* use IoU metric to match the remaining objects from high confidence to low confidence. Unmatched high confidence boxes are added to the tracking sequence as new tracking objects.

Algorithm 3 Pseudocode of the tracking process under TCBTrack architecture.

Input: image frame I^t , track indices $\mathcal{T}^{t-1} = \{\mathcal{T}_1^{t-1}, \mathcal{T}_2^{t-1}, \dots, \mathcal{T}_n^{t-1}\}$, model backbone Φ , detection head Ψ , ReID head Ω

- 1: Extract features $f^t = \Phi(I^t)$
- 2: $\mathcal{D}^t = \Psi(f^t), F^t = \Omega(f^t)$
- 3: $[\mathcal{D}_{high}^t, \mathcal{D}_{low}^t] \leftarrow \mathcal{D}^t, [F_{high}^t, F_{low}^t] \leftarrow F^t$
- 4: $\mathcal{T}^t \leftarrow Association1(\mathcal{T}^{t-1}, \mathcal{D}_{high}^t, F^t)$
- 5: $[\mathcal{D}_{remain}^t, \mathcal{T}_{remain}^{t-1}] \leftarrow [\mathcal{T}^t, \mathcal{T}^{t-1}, \mathcal{D}_{high}^t]$
- 6: $\mathcal{T}^t \leftarrow Association2(\mathcal{T}_{remain}^{t-1}, \mathcal{D}_{remain}^t) \cup \mathcal{T}^t$
- 7: $[\mathcal{T}_{remain}^t, \mathcal{D}_{remain}^t] \leftarrow [\mathcal{T}^t, \mathcal{T}_{remain}^{t-1}, \mathcal{D}_{remain}^t]$
- 8: $\mathcal{T}^t \leftarrow Association3(\mathcal{T}_{remain}^{t-1}, \mathcal{D}_{low}^t) \cup \mathcal{T}^t$
- 9: $[\mathcal{D}_{remain2}^t, \mathcal{T}_{remain2}^{t-1}] \leftarrow [\mathcal{T}^t, \mathcal{T}^{t-1}, \mathcal{D}_{low}^t]$
- 10: $[\mathcal{T}_{lost}^{t-1}, \mathcal{T}_{remove}^{t-1}] \leftarrow \mathcal{T}_{remain2}^{t-1}$
- 11: $\mathcal{T}_{new}^{t-1} \leftarrow \mathcal{D}_{remain}^t$
- 12: $\mathcal{T}^t \leftarrow \mathcal{T}_{lost}^{t-1} \cup \mathcal{T}_{new}^{t-1} \cup \mathcal{T}^t$
- 13: **return** \mathcal{T}^t

More detailed discussion of the hyper-parameters and the results on the data sets can be found in section 4.

4 Experiments

4.1 Implementation Details and Baseline Setup

4.1.1 Implementation of TCBTrack

We choose YOLOX-X as the detector for TCB-Track because it has an acceptable model size and because it is widely used. This simplifies the comparisons with other methods. To investigate the performance of the model under different detectors, we also utilize YOLO-S and YOLO-M as detectors to observe the tracking performance as detector capabilities are gradually decreased. We use the pretrained models released by ByteTrack/DanceTrack and only train the embedding head. For the models of MOT17 that are not public, we train on the combination of MOT17 half-training set and CrowdHuman dataset([Shao et al, 2018](#)). Building upon the experiments conducted with OMC, we introduce the DanceTrack dataset to examine the model’s robustness. This addition

is motivated by the fact that the MOT16/17/20 datasets predominantly consist of surveillance videos in which objects mostly move in a simple, linear manner. DanceTrack, on the other hand, provides a more complex dataset with objects exhibiting dramatic variations, irregular motions, and higher levels of similarity among objects, as it was collected from dance videos. In our experiments, we primarily explored the performance of cross-correlation learning in terms of robustness and accuracy, using the:

- Compare different training methods to demonstrate the advantages of cross-correlation learning in MOT tasks.
- Show that our enhanced association approach outperforms methods that primarily rely on IoU.
- Conduct comparisons with other trackers under high-speed conditions by sampling frames. We utilize the MOT17 dataset and DanceTrack dataset, which have frame rates of 25 fps and 20 fps respectively.

For MOT dataset, we divide the training dataset into two halves, using the first half(half-train) for training and the second half(half-val) for validation(See [Zhou et al \(2020\)](#)). Consequently, We choose to compare our tracker with other trackers that rely on motion cues to show the improvement to the MOT task brought by the generated temporal features.

For the training of the detection models, we employ the training parameters from YOLOX. For training embedding head, separate training is conducted using only the training sets from each dataset. The training involves 20 epochs with a batch size of 16. The initial learning rate was set to 1e-3, and the optimizer used was SGD with a weight decay of 5e-4 and a momentum of 0.9. The entire model is trained on four NVIDIA Tesla A100 GPUs, and all of the experiments are conducted on a single NVIDIA Tesla A100 GPU and Xeon(R) Gold 6146 3.20GHz CPU.

4.1.2 Metrics

We employ MOTA, FP, FN metrics from CLEAR([Bernardin and Stiefelhagen, 2008](#)) as our primary evaluation measures, supplemented by HOTA, AssA, DetA in [Luiten et al \(2021\)](#) and IDF1([Ristani et al, 2016](#)). By analysing FN and

Table 2 Analysis of different training methods on MOT17 half-val set and DanceTrack validation set. We also compare different ways of using feature distance metrics. When using linear weighting, we use grid search to search for the best weights and display the best results in the table.

Training	Association	MOT17			DanceTrack		
		MOTA↑	HOTA↑	IDF1↑	MOTA↑	HOTA↑	IDF1↑
ID Loss	Motion	77.8	68.0	80.0	86.3	46.1	50.9
	+Linear	77.6	67.8	80.0	87.3	46.1	51.0
	+Product	77.6	67.6	79.7	86.0	45.8	51.0
Ours	Motion	77.8	68.0	80.0	86.3	46.1	50.9
	+Linear	77.6	67.6	79.4	86.4	45.7	51.1
	+Product	77.6	67.7	79.7	88.1	47.9	53.7

FP, we can compare the number of false negatives and false positives produced by the models under different hyper-parameters. MOTA, derived from metrics such as FP and FN, is used to assess the detection quality and accuracy of the tracker. HOTA employs a more complex approach and is considered to be a more comprehensive measure of tracking performance. DetA, as the accuracy of detection, is also used to evaluate the performance of the detector; IDF1, AssA are utilized to evaluate the tracker’s association capabilities.

4.2 Experimental analyses of TCBTrack

4.2.1 Ablation study

We compare our training method with ID Loss. On the MOT17 dataset, using motion as the linear assignment weight already shows excellent results when the tracker incorporates Kalman filtering. When Kalman filtering can already address the issue, using features generated by the JDE tracker for association actually impairs tracking performance. However, as the dataset becomes more complex, our training method can provide more accurate association. Using equation (11), we can address the issue of inaccurate IoU scores to a greater extent. The results are shown in Table 2.

We investigate the effectiveness of our method for association. The results are shown in Table 3. Almost all Tracking-by-Detection paradigms currently rely on IoU scores of bounding boxes between consecutive frames as the primary weighting factor for the association algorithm. As mentioned in Zhang et al (2021), this is because factors such as size variations, lighting changes, and resolution in multi-object tracking make it

Table 3 Analysis of different association methods on DanceTrack validation set.

Association	HOTA	DetA	AssA	MOTA	IDF1
IoU	44.7	52.6	25.3	87.3	36.8
SORT	47.8	74.0	31.0	88.2	48.3
DeepSORT	45.8	70.9	29.7	87.1	46.8
MOTDT	39.2	68.8	22.5	84.3	39.6
BYTE	47.1	70.5	31.5	88.2	51.9
OC-SORT	52.1	79.8	35.3	87.3	51.6
Ours	54.6	78.9	38.0	89.9	54.7

Table 4 Analysis of the use of Kalman filter(K). Our association method has a similar performance without any prediction of the objects.

#NUM	K	MOTA↑	IDF1↑	FP↓	FN↓	IDs↓
1	✓	77.6	79.7	3436	9187	166
2		77.8	79.4	3403	9263	174

challenging to distinguish object features. Methods such as BYTE perform well on simple MOT datasets, they fail when there are large errors in estimates of the movements of objects. We provide a more robust methods for obtaining distance measure, furtherly improving the tracking performance.

To investigate the removal of Kalman filtering from our method, a comparative experiment is conducted on the MOT17 half-val set (The MOT17 contains pedestrians whose movements which can be estimated accurately using Kalman filtering), shown in Table 4. Our method compensates for the loss of IoU information, especially when the movements of the objects are large.

We also analyse the feature update strategy, with relevant results shown in Fig. 6. A smaller update weight improves association performance, as identity switch often happens when the object are close to other objects. A larger update weight

Table 5 Analysis of different backbones on MOT17 half-val set.

Detector	MOTA \uparrow	IDF1 \uparrow	HOTA \uparrow	Params \downarrow	GFLOPs \downarrow	FPS \uparrow
YOLOX-S	71.1	73.6	63.0	9.9M	90.07	58.5
YOLOX-M	74.5	76.2	65.4	27.4M	239.77	50.6
YOLO-X	77.6	79.3	67.5	104.7M	881.25	27.7

Table 6 Comparison with the state-of-the-art online MOT systems on DanceTrack benchmark. We assess a tracker’s real-time performance by evaluating whether its inference speed surpasses the frame rate of the dataset(20 fps). We report the corresponding official metrics. \uparrow/\downarrow indicate that higher/lower is better, respectively. The best scores for each method is marked in **bold**.

Method	HOTA \uparrow	DetA \uparrow	AssA \uparrow	MOTA \uparrow	IDF1 \uparrow
<i>Non-real-time:</i>					
CenterTrack(Zhou et al, 2020)	41.8	78.1	22.6	86.8	35.7
TransTrack(Sun et al, 2020)	45.5	75.9	27.5	88.4	45.2
GTR(Zhou et al, 2022)	48.0	72.5	31.9	84.7	50.3
StrongSORT++(Du et al, 2023)	55.6	80.7	38.6	91.1	55.2
Deep OC-SORT(Maggiolino et al, 2023)	61.3	82.2	45.8	92.3	61.5
MOTR(Zeng et al, 2022)	54.2	73.5	40.2	79.7	51.5
MOTRv2(Zhang et al, 2023)	73.4	83.7	64.4	92.1	76.0
<i>Online & real-time:</i>					
FairMOT(Zhang et al, 2021)	39.7	66.7	23.8	82.2	40.8
TraDes(Wu et al, 2021)	43.3	74.5	25.4	86.2	41.2
ByteTrack(Zhang et al, 2022)	47.7	71.0	32.1	89.6	53.9
QDTrack(Pang et al, 2021)	54.2	80.1	36.8	87.7	50.4
OC-SORT(Cao et al, 2023)	55.1	80.3	38.3	92.0	54.6
TCBTrack(Ours)	56.8	81.9	39.5	92.5	58.1
<i>Offline:</i>					
SUSHI(Cetintas et al, 2023)	63.3	80.1	50.1	88.7	63.4

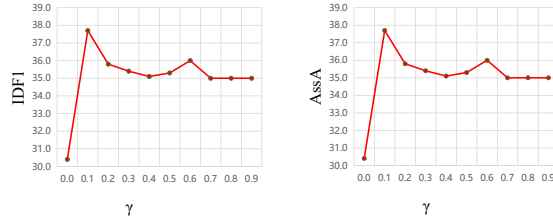


Fig. 6 Analysis of hyper-parameter γ mentioned in equation (14). Experiments are conducted on DanceTrack validation set.

introduces significant noise from similar background information, which is not suitable for our association method.

Furthermore, we investigate the feasibility of model lightweight. Table 5 presents the performance of TCBTrack on MOT17 half-val set at different scales. It is observed that even when

the detector becomes less accurate, our method still maintains tracking performance. For training sets such as MOT16, MOT17, DanceTrack, etc., we can achieve real-time requirements by lightweighting the detector. However, for the MOT20 dataset, we can only achieve online real-time performance by subsampling frames. This is because the MOT20 dataset contains a large number of objects in a single frame(up to around 200), causing tracking to consume a significant amount of time during the matching stage. This issue is also faced by all Tracking-by-Detection trackers. Possible solutions are: (1) Replace association with lightweight deep learning models. (2) Design a faster matching algorithm. This issue requires further exploration in future work. Currently, our model can address online and real-time tracking needs in most scenarios by model lightweight if necessary.

Table 7 Comparison with the state-of-the-art online MOT systems of different types under private detection on MOT17 benchmark. We assess a tracker’s real-time performance by evaluating whether its inference speed surpasses the average frame rate of the dataset(25 fps). We report the corresponding official metrics. \uparrow indicates that higher is better, \downarrow indicates that lower is better. The best scores for each method is marked in **bold**.

Method	HOTA \uparrow	MOTA \uparrow	IDF1 \uparrow	IDs \downarrow	FPS \uparrow
<i>Non-real-time:</i>					
Tracktor++(Bergmann et al, 2019)	44.8	56.3	55.1	1987	1.5
CTracker(Peng et al, 2020)	49.0	66.6	57.4	5529	6.8
TubeTK(Pang et al, 2020)	48.0	63.0	58.6	4137	3.0
UMA(Yin et al, 2020)	-	53.1	54.4	2251	5.0
CenterTrack(Zhou et al, 2020)	52.2	67.8	64.7	3039	17.5
SOTMOT(Zheng et al, 2021)	-	71.0	71.9	5184	16.0
TraDes(Wu et al, 2021)	52.7	69.1	63.9	3555	17.5
SiamMOT(Shuai et al, 2021)	-	76.3	72.3	-	12.8
QDTrack(Pang et al, 2021)	53.9	68.7	66.3	3378	20.3
CorrTracker(Wang et al, 2021a)	60.7	76.5	73.6	3369	15.6
CSTrack(Liang et al, 2022b)	59.3	74.9	72.6	3567	15.8
TransMOT(Chu et al, 2023)	-	76.7	75.1	2346	9.6
MOTR(Zeng et al, 2022)	57.8	73.4	68.6	2439	9.5
MOTRv2(Zhang et al, 2023)	62.0	78.6	75.0	-	6.9
BoT-SORT(Aharon et al, 2022)	64.6	80.6	79.5	1257	6.6
UTM(You et al, 2023)	64.0	81.8	78.7	1436	13.1
StrongSORT(Du et al, 2023)	63.5	78.3	78.5	1446	7.5
Deep OC-SORT(Maggiolino et al, 2023)	64.9	79.4	80.6	1023	<11.0
<i>Online & real-time:</i>					
SORT(Bewley et al, 2016)	34.0	43.1	39.8	4852	143.3
FairMOT(Zhang et al, 2021)	59.3	73.7	72.3	3303	25.9
ByteTrack(Zhang et al, 2022)	63.1	80.3	77.3	2196	29.6
OC-SORT(Cao et al, 2023)	63.2	78.0	77.5	1950	29.0
TCBTrack(Ours)	62.1	79.3	75.8	2157	27.7
<i>Offline:</i>					
MPNTrack(Brasó and Leal-Taixé, 2020)	49.0	58.8	61.7	1185	6.5
ReMOT(Yang et al, 2021)	59.7	77.0	72.0	2853	1.8
MAATrack(Stadler and Beyerer, 2022)	62.0	79.4	75.9	1452	189.1
SUSHI(Cetintas et al, 2023)	66.5	81.1	83.1	1149	14.2

4.2.2 Comparison with others

DanceTrack dataset. We compare TCBTrack with existing tracking methods on the DanceTrack test set. Table 6 shows that in the real-time tracker category, our method achieves state-of-the-art(SOTA) performance in metrics such as MOTA(+1.5), IDF1(+3.5), AssA(+1.2), and HOTA(+1.7). There is still some room for improvement to reach the current SOTA in non-real-time trackers. This is reasonable, because the trade-off between speed and accuracy inherently limits the achievable precision. In the existing SOTA, the most notable gap is observed between

MOTRv2 and other methods. Our analysis suggests that this discrepancy arises from the fact that all trackers use IoU as the positional information measure for candidate bounding boxes during the tracking phase. However, in practical scenarios, IoU can significantly affect object matching due to inaccurate outputs from the detector. A single erroneous match may cause failure in the tracking. MOTRv2 addresses this issue by leveraging the transformer network to obtain robust positional information for the objects. In future research, we will focus on enhancing the association stage of Tracking-by-Detection paradigm

Table 8 Comparison with the state-of-the-art online MOT systems using different paradigms under private detection on MOT20 benchmark. We report the corresponding official metrics. \uparrow indicates that higher is better, \downarrow indicates that lower is better. The best scores of methods are marked in **bold**.

Method	HOTA \uparrow	MOTA \uparrow	IDF1 \uparrow	IDs \uparrow	FPS \uparrow
<i>JDE paradigm:</i>					
FairMOT(Zhang et al, 2021)	54.6	61.8	67.3	5243	13.2
CSTrack(Liang et al, 2022b)	54.0	66.6	68.6	3196	4.5
GSDT(Wang et al, 2021b)	53.6	67.1	67.5	3131	0.9
CorrTracker(Wang et al, 2021a)	-	65.2	69.1	5183	8.5
RelationTrack(Yu et al, 2022)	56.5	67.2	70.5	4243	2.7
TCBTrack(ours)	60.6	76.0	74.4	1174	16.1
<i>SDE paradigm:</i>					
BoT-SORT-ReID(Aharon et al, 2022)	63.3	77.8	77.5	1257	2.4
StrongSORT(Du et al, 2023)	61.5	72.2	75.9	1066	1.5
Deep OC-SORT(Maggiolino et al, 2023)	63.9	75.6	79.2	779	<5.0
<i>Motion:</i>					
SORT(Bewley et al, 2016)	36.1	42.7	45.1	4470	57.3
ByteTrack(Zhang et al, 2022)	61.3	77.8	75.2	1223	17.5
OC-SORT(Cao et al, 2023)	62.1	75.5	75.9	913	-
MotionTrack(Qin et al, 2023)	62.8	78.0	76.5	1165	-
UCMCTrack(Yi et al, 2023)	62.8	75.6	77.4	1335	-
<i>Transformer paradigm:</i>					
MOTRv2(Zhang et al, 2023)	60.3	76.2	72.2	-	6.9
<i>Offline:</i>					
MPNTrack(Brasó and Leal-Taixé, 2020)	46.8	57.6	59.1	1210	6.5
ReMOT(Yang et al, 2021)	61.2	77.4	73.1	1789	0.4
MAATrack(Stadler and Beyerer, 2022)	57.3	73.9	71.2	1331	14.7
SUSHI(Cetintas et al, 2023)	64.3	74.3	79.8	706	<10.0
<i>Others:</i>					
SOTMOT(Zheng et al, 2021)	-	68.6	71.4	4209	8.5
UTM(You et al, 2023)	62.5	78.2	76.9	1228	6.2

trackers, aiming to achieve a true fusion of detection and tracking by improving the weighting scheme.

MOT dataset. We further validate the robustness of TCBTrack on different datasets by experimenting on MOT17(See Table 7) and MOT20(See Table 8). The tracking performance is on par with the best trackers across the board, which demonstrates the robustness of our approach. We have a slight performance gap (-2.8 HOTA, -0.1 MOTA, -4.8 IDF1) in MOT17 compared to Deep OC-SORT, a tracker that directly embeds the ReID model. However, we possess two distinct advantages over it: (1) Deep OC-SORT fails to achieve a balance between accuracy and speed due to its

reliance on both high-performing detectors and large ReID models. (2) We are able to avoid incorporating ID loss during tracker training, which enables us to train on larger datasets with the same training epochs. When compared to other methods that rely on motion, although our algorithm does not achieve significant improvement on these two datasets, we are still the first tracker to fully utilize temporal cues for matching in the association stage and achieve good performance. In addition, we have comprehensively analysed the experimental results for the MOT dataset and the DanceTrack dataset. Our TCBTrack is more robust, accurate, and lightweight than other current trackers in various scenarios. We believe that

Table 9 Comparison with the state-of-the-art online MOT systems on MOT17 “high-speed” dataset and DanceTrack “high-speed” dataset. We use ratios to show the fraction of the frames that are used. We report the corresponding official metrics. \uparrow indicates that higher is better, \downarrow indicates that lower is better. The best scores and the least decreasing scores of methods are marked in **bold**.

Method	Ratio	MOTA \uparrow	IDF1 \uparrow	HOTA \uparrow
MOT17				
SORT* ¹ (Bewley et al, 2016)	1.0	74.7	77.7	66.4
	0.5	71.2	76.4	64.9
	0.33	68.1(-6.6)	72.7(-5.0)	62.1(-4.3)
ByteTrack (Zhang et al, 2022)	1.0	77.8	80.0	68.0
	0.5	75.6	77.2	65.6
	0.33	73.9(-3.9)	74.2(-5.8)	63.7(-5.3)
OCSORT (Cao et al, 2023)	1.0	74.5	77.8	66.3
	0.5	71.4	76.6	65.1
	0.33	68.7(-5.8)	74.1(-3.7)	63.3(-3.0)
TCBTrack(ours)	1.0	77.6	79.3	67.5
	0.5	75.6	76.7	65.4
	0.33	73.7(-3.9)	74.3(-5.0)	63.4(-4.1)
DanceTrack				
SORT* ¹ (Bewley et al, 2016)	1.0	85.0	48.8	47.3
	0.5	81.8	44.3	41.9
	0.33	76.8(-8.2)	39.4(-9.4)	37.0(-10.3)
ByteTrack (Zhang et al, 2022)	1.0	86.3	46.1	50.9
	0.5	83.7	41.8	48.6
	0.33	80.3(-6.0)	39.1(-7.0)	44.8(-6.1)
OC-SORT (Cao et al, 2023)	1.0	87.3	52.1	51.6
	0.5	84.6	48.2	47.9
	0.33	80.8(-6.5)	44.2(-7.9)	42.8(-8.8)
TCBTrack(ours)	1.0	89.9	54.7	54.6
	0.5	88.8	52.1	53.4
	0.33	87.1(-2.8)	48.8(-5.8)	49.5(-5.1)

¹SORT*: We have replaced the detection head for SORT with YOLOX for fair comparison with other Tracking-by-Detection trackers.

temporal cues of the objects is still worth further investigation to achieve a better integration of ReID and MOT tasks.

Our modified dataset. Finally, we apply frame sampling to the MOT17 half-val dataset and DanceTrack validation set to construct a more difficult environment. As can be seen in Table 9, when evaluated on MOT17(0.33 ratio), our method achieves comparable performance(-0.2 MOTA, +0.1 IDF1, -0.3 HOTA) to those methods that rely on motion. Frame sampling



FairMOT*: We have replaced the detection head for FairMOT with YOLOX for fair comparison with other Tracking-by-Detection trackers.

Fig. 7 Analysis of TCBTrack compared with FairMOT and OC-SORT on our modified DanceTrack dataset (0.33 ratio). The arrows indicate errors in the tracking process, such as identity switching or identity loss.

has only a small effect. However, when evaluated on the DanceTrack dataset, the advantages of TCBTrack become apparent: we outperform other trackers under various tracking metrics(+7.3 MOTA, +4.6 IDF1, +4.7 HOTA) and the decrease in performance after frame sampling is relatively small. This demonstrates that TCBTrack handles objects moving irregularly at high speed. and with irregular patterns, proving the robustness of our association approach. Furthermore, as observed in both MOT17 and DanceTrack, TCBTrack performs well, even when 67% of frames are dropped. If necessary, TCBTrack can reduce the frame rate to meet the tracking task requirements for different choices of hardware.

We visualize the robustness analysis compared with other trackers, shown in Fig. 7. ByteTrack and OC-SORT, while leveraging advanced Kalman filtering, encounter tracking failures in complex scenarios due to inaccuracies in prediction. FairMOT, which employs JDE paradigm, is unable to make correct associations based on appearance features when faced with overlapping similar objects. Our TCBTrack effectively addresses the problem of appearance similarity and maintains high tracking accuracy and stability in complex scenes.

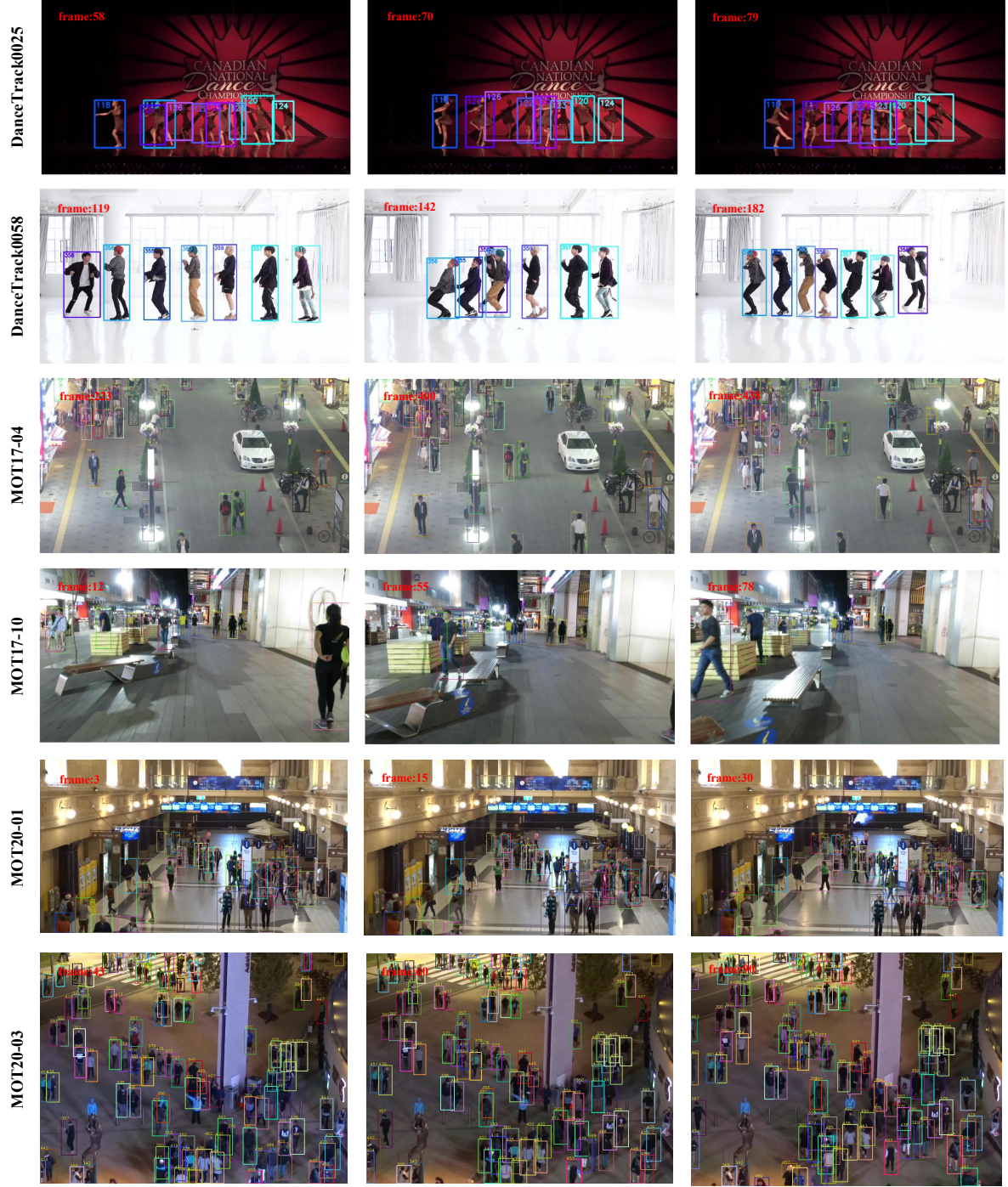


Fig. 8 Sample tracking results of TCBTrack on DanceTrack validation set, MOT17 validation set and MOT20 validation set. Each bounding box is assigned to a dedicated ID and color for differentiation.

Visualization. Fig. 8 presents some tracking results on the MOT17, MOT20 and DanceTrack datasets. From the figure, it can be observed that

our method effectively mitigates the impact of imprecise detector outputs. For example, in the first row of tracking results, ID 126 experiences

a detection deviation at frame 70 but continues to be correctly associated in subsequent frames. Our method also addresses occlusion issues, as illustrated in the second row of visualizations where the leftmost person passes behind six other persons with significant occlusion. Finally, on the MOT17 dataset and MOT20 dataset, we demonstrate that our tracker performs robustly in various scenarios with different perspectives and resolutions, maintaining accurate object tracking.

5 Conclusion

In this paper, we explore the importance of temporal cues in MOT tasks, arguing that incorporating temporal information enhances object feature association, leading to improved performance across various datasets. By incorporating the JDE paradigm and cross-correlation learning in the training process, TCBTrack enhances the quality of object features. Our experimental results on various datasets show effectiveness of TCBTrack. To simulate a more difficult tracking environment, we employ two strategies: detector lightweighting and dataset frame sampling. We then compare our approach, TCBTrack, with other state-of-the-art trackers to show its superiority in online and in real time performance. Through these comprehensive experiments, we demonstrate that our model is a robust and high-speed tracker, achieving top performance in online tracking scenarios. Overall, we believe that our work is a significant contribution to MOT that emphasises the role of temporal cues and presenting a versatile tracking system that strikes a balance between speed and accuracy.

References

Aharon N, Orfaig R, Bobrovsky BZ (2022) Bot-sort: Robust associations multi-pedestrian tracking. arXiv preprint arXiv:220614651

Bergmann P, Meinhardt T, Leal-Taixé L (2019) Tracking without bells and whistles. In: Proceedings of the IEEE/CVF International Conference on Computer Vision, pp 941–951

Bernardin K, Stiefelhagen R (2008) Evaluating multiple object tracking performance: the clear mot metrics. EURASIP Journal on Image and Video Processing 2008:1–10

Bertinetto L, Valmadre J, Henriques JF, et al (2016) Fully-convolutional siamese networks for object tracking. In: Computer Vision–ECCV 2016 Workshops: Amsterdam, The Netherlands, October 8–10 and 15–16, 2016, Proceedings, Part II 14, Springer, pp 850–865

Bewley A, Ge Z, Ott L, et al (2016) Simple online and realtime tracking. In: 2016 IEEE international conference on image processing (ICIP), IEEE, pp 3464–3468

Bochinski E, Eiselein V, Sikora T (2017) High-speed tracking-by-detection without using image information. In: 2017 14th IEEE international conference on advanced video and signal based surveillance (AVSS), IEEE, pp 1–6

Bochinski E, Senst T, Sikora T (2018) Extending iou based multi-object tracking by visual information. In: 2018 15th IEEE International Conference on Advanced Video and Signal Based Surveillance (AVSS), IEEE, pp 1–6

Brasó G, Leal-Taixé L (2020) Learning a neural solver for multiple object tracking. In: Proceedings of the IEEE/CVF conference on computer vision and pattern recognition, pp 6247–6257

Cao J, Pang J, Weng X, et al (2023) Observation-centric sort: Rethinking sort for robust multi-object tracking. In: Proceedings of the IEEE/CVF Conference on Computer Vision and Pattern Recognition, pp 9686–9696

Carion N, Massa F, Synnaeve G, et al (2020) End-to-end object detection with transformers. In: European conference on computer vision, Springer, pp 213–229

Cetintas O, Brasó G, Leal-Taixé L (2023) Unifying short and long-term tracking with graph hierarchies. In: Proceedings of the IEEE/CVF Conference on Computer Vision and Pattern Recognition, pp 22877–22887

Chen L, Ai H, Zhuang Z, et al (2018) Real-time multiple people tracking with deeply learned candidate selection and person re-identification. In: 2018 IEEE international conference on multimedia and expo (ICME), IEEE, pp 1–6

Chu P, Wang J, You Q, et al (2023) Transmot: Spatial-temporal graph transformer for multiple object tracking. In: Proceedings of the IEEE/CVF Winter Conference on Applications of Computer Vision, pp 4870–4880

Chu Q, Ouyang W, Li H, et al (2017) Online multi-object tracking using cnn-based single object tracker with spatial-temporal attention mechanism. In: Proceedings of the IEEE international conference on computer vision, pp 4836–4845

Cui Y, Zeng C, Zhao X, et al (2023) Sportsmot: A large multi-object tracking dataset in multiple sports scenes. arXiv preprint arXiv:230405170

Dai P, Weng R, Choi W, et al (2021) Learning a proposal classifier for multiple object tracking. In: Proceedings of the IEEE/CVF Conference on Computer Vision and Pattern Recognition, pp 2443–2452

Dendorfer P, Rezatofighi H, Milan A, et al (2020) Mot20: A benchmark for multi object tracking in crowded scenes. arXiv preprint arXiv:200309003

Dosovitskiy A, Beyer L, Kolesnikov A, et al (2020) An image is worth 16x16 words: Transformers for image recognition at scale. arXiv preprint arXiv:201011929

Du Y, Zhao Z, Song Y, et al (2023) Strongsort: Make deepsort great again. IEEE Transactions on Multimedia

Gao R, Wang L (2023) Memotr: Long-term memory-augmented transformer for multi-object tracking. In: Proceedings of the IEEE/CVF International Conference on Computer Vision, pp 9901–9910

Ge Z, Liu S, Wang F, et al (2021) Yolox: Exceeding yolo series in 2021. arXiv preprint arXiv:210708430

Geiger A, Lenz P, Stiller C, et al (2013) Vision meets robotics: The kitti dataset. The International Journal of Robotics Research 32(11):1231–1237

Girshick R (2015) Fast r-cnn. In: Proceedings of the IEEE international conference on computer vision, pp 1440–1448

Gu R, Wang G, Hwang JN (2019) Efficient multi-person hierarchical 3d pose estimation for autonomous driving. In: 2019 IEEE Conference on Multimedia Information Processing and Retrieval (MIPR), IEEE, pp 163–168

Hatamizadeh A, Tang Y, Nath V, et al (2022) Unetr: Transformers for 3d medical image segmentation. In: Proceedings of the IEEE/CVF winter conference on applications of computer vision, pp 574–584

He K, Gkioxari G, Dollár P, et al (2017) Mask r-cnn. In: Proceedings of the IEEE international conference on computer vision, pp 2961–2969

He M, Takeuchi E, Ninomiya Y, et al (2016) Precise and efficient model-based vehicle tracking method using rao-blackwellized and scaling series particle filters. In: 2016 IEEE/RSJ international conference on intelligent robots and systems (IROS), IEEE, pp 117–124

Kalman RE, et al (1960) Contributions to the theory of optimal control. Bol soc mat mexicana 5(2):102–119

Kim A, Brasó G, Ošep A, et al (2022) Polarmot: How far can geometric relations take us in 3d multi-object tracking? In: European Conference on Computer Vision, Springer, pp 41–58

Kuhn HW (1955) The hungarian method for the assignment problem. Naval research logistics quarterly 2(1-2):83–97

Li B, Yan J, Wu W, et al (2018) High performance visual tracking with siamese region proposal network. In: Proceedings of the IEEE conference on computer vision and pattern recognition, pp 8971–8980

Li B, Wu W, Wang Q, et al (2019) Siamrpn++: Evolution of siamese visual tracking with very deep networks. In: Proceedings of the IEEE/CVF conference on computer vision and pattern recognition, pp 4282–4291

Li J, Gao X, Jiang T (2020) Graph networks for multiple object tracking. In: Proceedings of the IEEE/CVF winter conference on applications of computer vision, pp 719–728

Li Y, Yu Z, Phlion J, et al (2023) End-to-end 3d tracking with decoupled queries. In: Proceedings of the IEEE/CVF International Conference on Computer Vision, pp 18302–18311

Liang C, Zhang Z, Zhou X, et al (2022a) One more check: making “fake background” be tracked again. In: Proceedings of the AAAI Conference on Artificial Intelligence, pp 1546–1554

Liang C, Zhang Z, Zhou X, et al (2022b) Rethinking the competition between detection and reid in multiobject tracking. *IEEE Transactions on Image Processing* 31:3182–3196

Lin TY, Dollár P, Girshick R, et al (2017a) Feature pyramid networks for object detection. In: Proceedings of the IEEE conference on computer vision and pattern recognition, pp 2117–2125

Lin TY, Goyal P, Girshick R, et al (2017b) Focal loss for dense object detection. In: Proceedings of the IEEE international conference on computer vision, pp 2980–2988

Liu H, Abbeel P (2024) Blockwise parallel transformers for large context models. *Advances in Neural Information Processing Systems* 36

Liu H, Zaharia M, Abbeel P (2023a) Ring attention with blockwise transformers for near-infinite context. arXiv preprint arXiv:231001889

Liu Q, Chu Q, Liu B, et al (2020) Gsm: Graph similarity model for multi-object tracking. In: IJCAI, pp 530–536

Liu Z, Wang X, Wang C, et al (2023b) Sparse-track: Multi-object tracking by performing scene decomposition based on pseudo-depth. arXiv preprint arXiv:230605238

Lu Z, Rathod V, Votell R, et al (2020) Retinatrack: Online single stage joint detection and tracking. In: Proceedings of the IEEE/CVF conference on computer vision and pattern recognition, pp 14668–14678

Luiten J, Osep A, Dendorfer P, et al (2021) Hota: A higher order metric for evaluating multi-object tracking. *International journal of computer vision* 129:548–578

Luo C, Yang X, Yuille A (2021) Exploring simple 3d multi-object tracking for autonomous driving. In: Proceedings of the IEEE/CVF International Conference on Computer Vision, pp 10488–10497

Maggiolino G, Ahmad A, Cao J, et al (2023) Deep oc-sort: Multi-pedestrian tracking by adaptive re-identification. arXiv preprint arXiv:230211813

Mahalanobis PC (2018) On the generalized distance in statistics. *Sankhyā: The Indian Journal of Statistics, Series A* (2008-) 80:S1–S7

Milan A, Leal-Taixé L, Reid I, et al (2016) Mot16: A benchmark for multi-object tracking. arXiv preprint arXiv:160300831

Pang B, Li Y, Zhang Y, et al (2020) Tubetk: Adopting tubes to track multi-object in a one-step training model. In: Proceedings of the IEEE/CVF conference on computer vision and pattern recognition, pp 6308–6318

Pang J, Qiu L, Li X, et al (2021) Quasi-dense similarity learning for multiple object tracking. In: Proceedings of the IEEE/CVF conference on computer vision and pattern recognition, pp 164–173

Papakis I, Sarkar A, Karpatne A (2020) Gcnnmatch: Graph convolutional neural networks for multi-object tracking via sinkhorn normalization. arXiv preprint arXiv:201000067

Peng J, Wang C, Wan F, et al (2020) Chained-tracker: Chaining paired attentive regression results for end-to-end joint multiple-object detection and tracking. In: Computer Vision–ECCV 2020: 16th European Conference, Glasgow, UK, August 23–28, 2020, Proceedings, Part IV 16, Springer, pp 145–161

Petrovskaya A, Thrun S (2009) Model based vehicle detection and tracking for autonomous urban driving. *Autonomous Robots* 26(2-3):123–139

Qin Z, Zhou S, Wang L, et al (2023) Motion-track: Learning robust short-term and long-term motions for multi-object tracking. In: Proceedings of the IEEE/CVF conference on computer vision and pattern recognition, pp 17939–17948

Redmon J, Farhadi A (2018) Yolov3: An incremental improvement. arXiv preprint arXiv:180402767

Ren S, He K, Girshick R, et al (2015) Faster r-cnn: Towards real-time object detection with region proposal networks. *Advances in neural information processing systems* 28

Ristani E, Solera F, Zou R, et al (2016) Performance measures and a data set for multi-target, multi-camera tracking. In: European conference on computer vision, Springer, pp 17–35

Sadeghian A, Alahi A, Savarese S (2017) Tracking the untrackable: Learning to track multiple cues with long-term dependencies. In: Proceedings of the IEEE international conference on computer vision, pp 300–311

Schroff F, Kalenichenko D, Philbin J (2015) Facenet: A unified embedding for face recognition and clustering. In: Proceedings of the IEEE conference on computer vision and pattern recognition, pp 815–823

Shao S, Zhao Z, Li B, et al (2018) Crowdhuman: A benchmark for detecting human in a crowd. arXiv preprint arXiv:180500123

Shuai B, Berneshawi A, Li X, et al (2021) Siammot: Siamese multi-object tracking. In: Proceedings of the IEEE/CVF conference on computer vision and pattern recognition, pp 12372–12382

Stadler D, Beyerer J (2022) Modelling ambiguous assignments for multi-person tracking in crowds. In: Proceedings of the IEEE/CVF winter conference on applications of computer vision, pp 133–142

Sun P, Cao J, Jiang Y, et al (2020) Transtrack: Multiple object tracking with transformer. arXiv preprint arXiv:201215460

Sun P, Cao J, Jiang Y, et al (2022) Dancetrack: Multi-object tracking in uniform appearance and diverse motion. In: Proceedings of the IEEE/CVF Conference on Computer Vision and Pattern Recognition, pp 20993–21002

Tang S, Andriluka M, Andres B, et al (2017) Multiple people tracking by lifted multicut and person re-identification. In: Proceedings of the IEEE conference on computer vision and pattern recognition, pp 3539–3548

Varior RR, Shuai B, Lu J, et al (2016) A siamese long short-term memory architecture for human re-identification. In: Computer Vision–ECCV 2016: 14th European Conference, Amsterdam, The Netherlands, October 11–14, 2016, Proceedings, Part VII 14, Springer, pp 135–153

Wang Q, Zheng Y, Pan P, et al (2021a) Multiple object tracking with correlation learning. In: Proceedings of the IEEE/CVF Conference on Computer Vision and Pattern Recognition, pp 3876–3886

Wang Y, Kitani K, Weng X (2021b) Joint object detection and multi-object tracking with graph neural networks. In: 2021 IEEE International Conference on Robotics and Automation (ICRA), IEEE, pp 13708–13715

Wang YH (2022) Smiletrack: Similarity learning for multiple object tracking. arXiv preprint arXiv:221108824

Wang Z, Zheng L, Liu Y, et al (2020) Towards real-time multi-object tracking. In: European Conference on Computer Vision, Springer, pp 107–122

Wojke N, Bewley A, Paulus D (2017) Simple online and realtime tracking with a deep association metric. In: 2017 IEEE international conference on image processing (ICIP), IEEE, pp 3645–3649

Wu J, Cao J, Song L, et al (2021) Track to detect and segment: An online multi-object tracker. In: Proceedings of the IEEE/CVF conference on computer vision and pattern recognition, pp 12352–12361

Wu Y, Kong D, Wang S, et al (2019) An unsupervised real-time framework of human pose tracking from range image sequences. *IEEE Transactions on Multimedia* 22(8):2177–2190

Yang F, Chang X, Sakti S, et al (2021) Remot: A model-agnostic refinement for multiple object tracking. *Image and Vision Computing* 106:104091

Yang M, Han G, Yan B, et al (2023) Hybrid-sort: Weak cues matter for online multi-object tracking. *arXiv preprint arXiv:230800783*

Yi K, Luo K, Luo X, et al (2023) Ucmctrack: Multi-object tracking with uniform camera motion compensation. *arXiv preprint arXiv:231208952*

Yin J, Wang W, Meng Q, et al (2020) A unified object motion and affinity model for online multi-object tracking. In: Proceedings of the IEEE/CVF Conference on Computer Vision and Pattern Recognition, pp 6768–6777

You S, Yao H, Bao Bk, et al (2023) Utm: A unified multiple object tracking model with identity-aware feature enhancement. In: Proceedings of the IEEE/CVF Conference on Computer Vision and Pattern Recognition, pp 21876–21886

Yu E, Li Z, Han S, et al (2022) Relationtrack: Relation-aware multiple object tracking with decoupled representation. *IEEE Transactions on Multimedia*

Yu E, Wang T, Li Z, et al (2023) Motrv3: Release-fetch supervision for end-to-end multi-object tracking. *arXiv preprint arXiv:230514298*

Yu F, Li W, Li Q, et al (2016a) Poi: Multiple object tracking with high performance detection and appearance feature. In: Computer Vision–ECCV 2016 Workshops: Amsterdam, The Netherlands, October 8–10 and 15–16, 2016, Proceedings, Part II 14, Springer, pp 36–42

Yu F, Chen H, Wang X, et al (2020) Bdd100k: A diverse driving dataset for heterogeneous multitask learning. In: Proceedings of the IEEE/CVF conference on computer vision and pattern recognition, pp 2636–2645

Yu J, Jiang Y, Wang Z, et al (2016b) Unitbox: An advanced object detection network. In: Proceedings of the 24th ACM international conference on Multimedia, pp 516–520

Zeng F, Dong B, Zhang Y, et al (2022) Motr: End-to-end multiple-object tracking with transformer. In: European Conference on Computer Vision, Springer, pp 659–675

Zhai X, Kolesnikov A, Houlsby N, et al (2022) Scaling vision transformers. In: Proceedings of the IEEE/CVF Conference on Computer Vision and Pattern Recognition, pp 12104–12113

Zhang H, Yu Y, Jiao J, et al (2019) Theoretically principled trade-off between robustness and accuracy. In: International conference on machine learning, PMLR, pp 7472–7482

Zhang Y, Wang C, Wang X, et al (2021) Fairmot: On the fairness of detection and re-identification in multiple object tracking. *International Journal of Computer Vision* 129:3069–3087

Zhang Y, Sun P, Jiang Y, et al (2022) Byte-track: Multi-object tracking by associating every detection box. In: European Conference on Computer Vision, Springer, pp 1–21

Zhang Y, Wang T, Zhang X (2023) Motrv2: Bootstrapping end-to-end multi-object tracking by pretrained object detectors. In: Proceedings of the IEEE/CVF Conference on Computer Vision and Pattern Recognition, pp 22056–22065

Zheng L, Tang M, Chen Y, et al (2021) Improving multiple object tracking with single object tracking. In: Proceedings of the IEEE/CVF Conference on Computer Vision and Pattern Recognition, pp 2453–2462

Zhou X, Koltun V, Krähenbühl P (2020) Tracking objects as points. In: European conference on computer vision, Springer, pp 474–490

Zhou X, Yin T, Koltun V, et al (2022) Global tracking transformers. In: Proceedings of the IEEE/CVF Conference on Computer Vision and Pattern Recognition, pp 8771–8780

Zhu J, Yang H, Liu N, et al (2018) Online multi-object tracking with dual matching attention networks. In: Proceedings of the European

conference on computer vision (ECCV), pp 366–382